



**BUDAPEST UNIVERSITY OF TECHNOLOGY AND ECONOMICS
FACULTY OF CHEMICAL AND BIOCHEMICAL ENGINEERING
GYÖRGY OLÁH DOCTORAL SCHOOL**

Enhancing the enantiomeric purity of scalemic mixtures by
gas antisolvent fractionation

PhD thesis booklet

Author: Márton Kőrösi
Supervisor: Dr. Edit Székely

Department of Chemical and Environmental Process Engineering

2020.

1. Introduction and objectives

Recrystallization-based enantiomeric enrichment at ambient pressure is well established. Chiral compounds can be divided into three groups based on the (secondary) interactions among their molecules (i.e. conglomerates, racemic compounds and solid solutions).¹ Conglomerate forming chiral chemicals are described with strong interaction (e.g. H-bonds) between their molecules of the same enantiomer and significantly weaker interactions between the antipodes. Racemic compounds – the group of molecules some members of which I investigated in my PhD research work – can be characterized by the domination of the intermolecular interaction between the different enantiomers of the same molecule. Solid solutions exhibit similar homo- and heterochiral interactions. The melting behavior of chiral compounds (schematically pictured in *Figure 1*) provides information about the chiral characteristic of a certain compound.

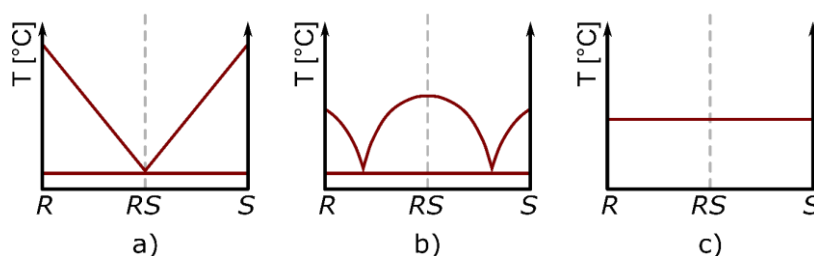


Figure 1 – General melting phase diagrams of chiral compounds. a) Melting diagram of a conglomerate forming chemical b) Melting diagram of a racemic compound c) Melting diagram of a solid solution.

For example, racemic compounds show two melting eutectics. These are located symmetrically around the racemic composition. In the case of recrystallization-based purification, the solid-phase behavior of the compounds – influencing the shape of the melting phase diagrams – also has a decisive role, regardless of whether crystallization is carried out from a melt or from a solution, provided that thermodynamic control determines the composition of the products. When crystallizing racemic compounds, the composition of the products is strongly influenced by the relative values of the composition (i.e. enantiomeric purity) of the starting material and the eutectic composition. Starting from a mixture having lower than eutectic ee ², the melt or mother liquor will be enriched in the major enantiomer while a less pure crystalline product is obtained. When initial enantiomeric purity exceeds the eutectic composition, the behavior is

¹ F. Faigl, E. Fogassy, M. Nógrádi, E. Pálovics, J. Schindler, Separation of non-racemic mixtures of enantiomers: an essential part of optical resolution, *Org. Biomol. Chem.* 8 (2010) 947-959. doi:10.1039/b917564d.

² $ee = \left| \frac{Q_R - Q_S}{Q_R + Q_S} \right|$, where Q refers to the concentration of the enantiomers of a molecule, the configuration of which is described by the indices.

more favorable: the major enantiomer accumulates in the crystalline phase leaving behind a melt or mother liquor closer to racemic composition.

Supercritical carbon dioxide is a modern alternative to organic solvents, owing to its tunable properties and non-hazardous nature. Its application might enable the synthesis of products with unique properties, and its large-scale industrial applications have also been developed.³ Optically active or enantiomerically pure products are good candidates for products with sufficient added value to make supercritical fluid extraction, antisolvent precipitation processes or reactions done in a supercritical medium economically feasible. Simándi, Fogassy and their colleagues described a very high selectivity in case of half molar equivalent resolutions using supercritical carbon dioxide as an extraction solvent. The reason was the very high difference between the solubility values of the salts and the unreacted compounds.⁴ Since then, our research group has explored the possibilities of using supercritical carbon dioxide as a solvent in the heterogeneous phase reaction of racemates and resolving agents⁵, resolving agents formed with carbon dioxide in the autoclave⁶, and enzymatic kinetic resolutions⁷. Also, carbon dioxide was applied in a very different role: as an antisolvent in enantioselective precipitation experiments.⁸ In case of gas antisolvent fractionation – the batch precipitation operation used in the current work – an organic solution of a target compound is mixed with high-pressure carbon dioxide. The major steps of the process are summarized in *Figure 2*. During pressurization, carbon dioxide is mixed with the organic solvent. The organic solvent is usually more polar, and, as a result of the quantity of carbon dioxide increasing it loses both polarity and dissolving power. Pressurization continues until a biphasic system is obtained, consisting of the precipitated solids and a solution. The still dissolved components are extracted together with the original organic solvent using pure supercritical carbon dioxide.

³ Ž. Knez, E. Markočič, M. Leitgeb, M. Primožič, M. Knez Hrnčič, M. Škerget, Industrial applications of supercritical fluids: A review, *Energy*. 77 (2014) 235–243. doi:10.1016/j.energy.2014.07.044.

⁴ E. Fogassy, M. Ács, T. Szili, B. Simándi, J. Sawinsky, Molecular chiral recognition in supercritical solvents, *Tetrahedron Lett.* 35 (1994) 257–260. doi:10.1016/S0040-4039(00)76525-7.

⁵ G. Bántóghy, E. Székely, D.M. Sevillano, Z. Juvancz, B. Simándi, Diastereomer salt formation of ibuprofen in supercritical carbon dioxide, *J. Supercrit. Fluids*. 69 (2012) 113–116. doi:10.1016/J.SUPFLU.2012.05.016.

⁶ L. Lőrincz, Z. Hovonyecz, J. Madarász, E. Varga, E. Székely, Resolution of ibuprofen with primary amine carbamates in supercritical carbon dioxide, *Period. Polytech. Chem. Eng.* 63 (2019) 312–317. doi:10.3311/PPCh.12918.

⁷ E. Székely, M. Utczás, B. Simándi, Kinetic enzymatic resolution in scCO₂ – Design of continuous reactor based on batch experiments, *J. Supercrit. Fluids*. 79 (2013) 127–132. doi:10.1016/J.SUPFLU.2012.11.016.

⁸ G. Bántóghy, L. Lőrincz, I.M. Szilágyi, J. Madarász, E. Székely, Crystallization and Resolution of cis-Permethric Acid with Carbon Dioxide Antisolvent, *Chem. Eng. Technol.* 37 (2014) 1417–1421. doi:10.1002/ceat.201300718.

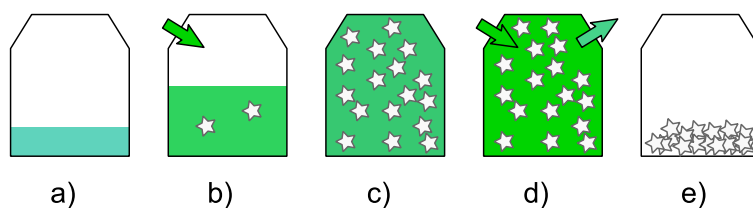


Figure 2 – A schematic depiction of the main steps of the GAS process. a) The compound to be precipitated is dissolved in an organic solvent and filled into the high-pressure vessel. b) Carbon dioxide is introduced, resulting in the organic solvent swelling and losing dissolving power. c) Pressurization is continued until a homogenous solvent mixture is reached. Crystallization is completed during this equilibration phase. d) The organic solvent and any dissolved compounds are extracted using pure carbon dioxide. e) A dry, micronized product can be collected after depressurization.

The application of gas antisolvent fractionation for the enantiomeric enrichment of non-racemates (also called scalemic mixtures) has not been previously studied, while the detailed studies on the recrystallization of diastereomeric mixtures is also lacking⁹. The aim of my PhD research is thus the systematic studying of enantiomeric enrichment via the recrystallization of diastereomeric salts and scalemic enantiomeric mixtures using gas antisolvent fractionation as the separation method. In the investigations on scalemic acids, 2-, 3- and 4- chloromandelic acids were chosen as model molecules while the recrystallization of diastereomeric salts was studied on the example of the 1-phenylethanammonium salts of mandelic acid and 4-chloromandelic acid. My aim was to investigate the effect of the initial enantiomeric or diastereomeric composition on the products' purity. The results were compared to the atmospheric melting phase diagrams of the chemicals. In order to gain a better understanding of the correlation between the high pressure crystallization results and the phase diagram recorded at ambient pressure, the melting behavior of the chlorinated mandelic acids and the salt of 4-chloromandelic acid and 1-phenylethanamine was investigated under high carbon dioxide pressure. My aim was to experimentally investigate the chiral melting phase diagrams and, to investigate whether the simple equations widely used in the calculation of atmospheric melting phase diagrams are also applicable for high pressure systems containing carbon dioxide.

⁹ Kordikowski, A., York, P., & Latham, D. (1999). Resolution of ephedrine in supercritical CO₂: A novel technique for the separation of chiral drugs. *Journal of Pharmaceutical Sciences*, 88(8), 786–791. <https://doi.org/10.1021/js980459f>

2. Experimental methods

2.1. Gas antisolvent fractionation (GASF)

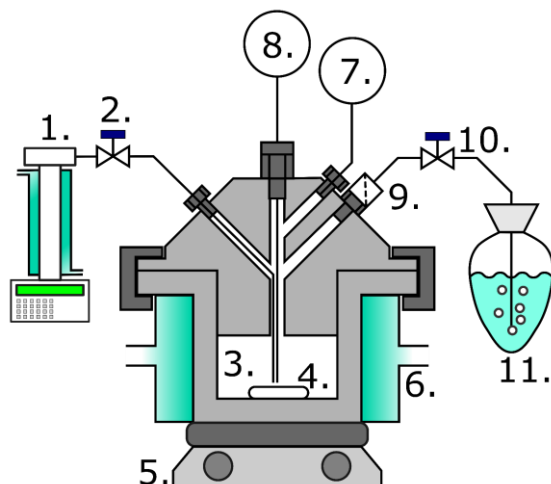


Figure 3 – A non-proportional, schematic depiction of the laboratory autoclave used in the GASF experiments. 1. Teledyne ISCO 260D syringe pump; 2. Inlet valve; 3. An inlet tube leading towards the bottom of the reactor vessel; 4. Magnetic stirrer; 5. Magnetic motor (without heating); 6. Heating jacket with circulating water; 7. Pressure gauge and transducer; 8. Thermocouple; 9. Filter; 10. Outlet valve; 11. Solvent trap

GAS antisolvent precipitation experiments were carried out in a laboratory scale high pressure reactor depicted in *Figure 3*. Generally, gas antisolvent fractionation experiments begin with tempering the reactor and adding a homogeneous solution of the compounds in an organic solvent. After assembling the reactor (i.e. mounting the top of the reactor and all of the valves and transducers) it is pressurized. The used Teledyne ISCO 260D pump has a syringe-like cylinder that can be filled with liquid carbon dioxide. It is tempered using a thermostat circulating water so that the carbon dioxide inside is always in liquid state. The pump can actuate the piston inside its cylinder to either operate at constant pressure, or to deliver a constant volumetric flow rate.

In the experiments discussed in this work, the pump was always operated in constant pressure mode. The reactor is pressurized through a regulating valve. Carbon dioxide passes through a tube towards the bottom of the reactor, ensuring thorough mixing during pressurization and extraction. The mixture is stirred by a magnetic mixer. The reactor is tempered using a jacket with water circulating through it. Stirring is started when the operational pressure specified by the experiment is reached. Operational parameters in the reactor were recorded by a computer data logging system. After some equilibration time, the extraction of the dissolved components and the organic solvent is carried out using pure carbon dioxide. Solid particles were kept from being washed out of the reactor during the extraction phase by a sintered metallic filter. The flowrate of CO₂ was regulated by the outlet valve. A solvent trap was used to recover the extracted compounds. The outlet valve and the pipe connecting it to the solvent trap were rinsed after depressurization. After disassembling the reactor, the crystalline product was collected from the high pressure vessel in solid form. In order to improve recovery, solid residue was

collected from the vessel using a small amount of organic solvent. The resulting solution, as well as the solution collected from the solvent trap (containing the extract) were evaporated using a rotational vacuum distiller. *Figure 4.* shows the scheme of diastereomeric salt recrystallization experiments and the chlorinated mandelic acid derivatives the scalemic mixtures of which were recrystallized.

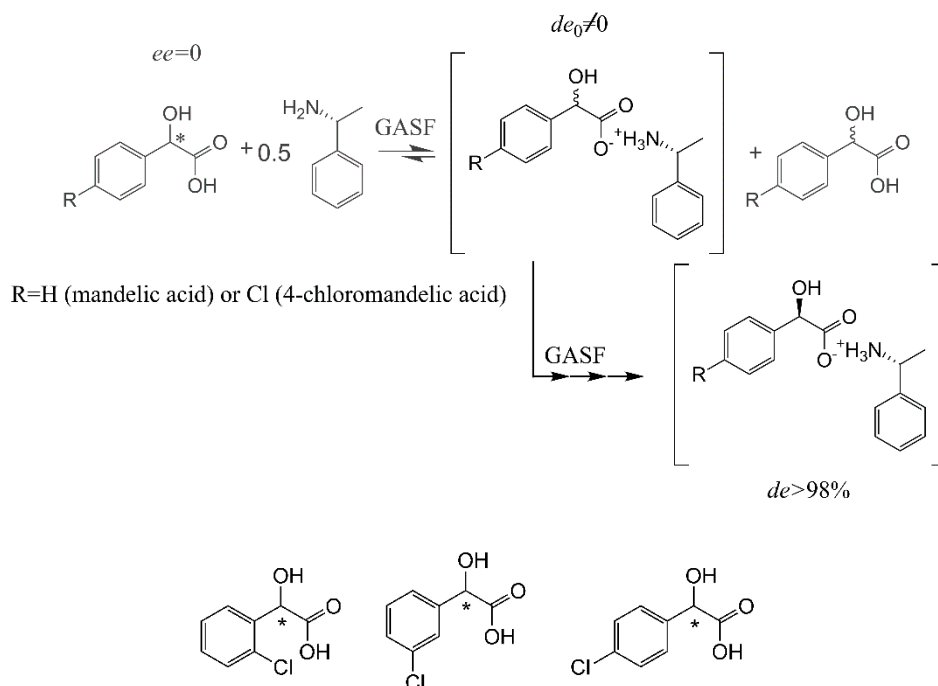


Figure 4 – Reaction and constitutional schemes of the recrystallization of the 1-phenylethanammonium salts of mandelic acid and 4-chloromandelic acid, and the chosen chlorinated mandelic acid derivatives (from left to right 2-, 3- and 4-chloromandelic acid)

2.2. Phase equilibrium measurements using a high-pressure view-cell

A Pickel's cell (New Ways of Analytics GmbH.) was used for these experiments, a schematic depiction of which is shown in *Figure 5*. The drawing shows the configuration used in high pressure melting experiments, an almost identical equipment was used in my research work for solubility measurements. These were carried out by recording cloud and redissolution points. The vessel has two sapphire windows, so the sample inside the cell can be illuminated and observed visually. The rear wall of the cylindrical cell is a piston allowing adjustments to its volume, thus pressure can be varied (or kept constant) independently from other operational parameters. The apparatus is a versatile tool for visually observing processes (such as crystallizations or spray nozzle jets) or measuring equilibria in a high pressure environment.

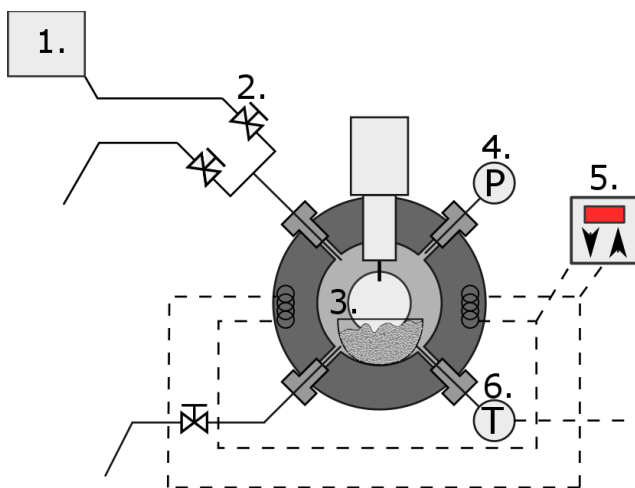


Figure 5 – A schematic, cross sectional depiction of the view cell used in the experiments. 1. Pickel module (CO₂ pump); 2. Valve regulating the rate of pressurization; 3. Sample placed in glass sample holder in front of the movable piston of the apparatus; 4. Pressure gauge; 5. Temperature regulator; 6. Temperature transducer

Melting point measurements were carried out at the Ruhr-University Bochum. During the measurements, a sample of crystalline material was placed in a glass sample holder, which was then loaded into the view cell. It was stacked up against the wall of the sample holder facing the sapphire window of the cell. The apparatus was closed and set to minimal volume, and preheated. Video recording was started and the equipment was pressurized with carbon dioxide using a high pressure pump. Pressure was elevated slowly

in order to maintain a constant temperature and to avoid dislodging the crystalline particles from the sample holder. After reaching operational pressure, temperature was slowly increased. The pressure elevation caused by the expansion of carbon dioxide on increasing temperature was compensated by increasing the volume of the cell. Melting was observed visually as well as recorded. Temperature values were noted on observing the first droplet of liquid or the first small change in the sample volume. A second value was recorded when a larger change in the sample volume was noticed, and finally the temperature needed to completely melt the sample was noted. Afterwards, the cell was depressurized and cooled to ambient temperature.

2.4. High-pressure DSC measurements

The equipment used was a Setaram C80 Calvet Calorimeter coupled with a Red Lion syringe pump. At the beginning, the pump was filled with carbon dioxide from a gas cylinder. Known masses of the powdered samples (roughly 50-100 mg) were filled into a stainless steel sample holder which, together with an empty reference, was placed in the calorimeter. After rinsing the cells with carbon dioxide, they were filled with supercritical carbon dioxide to the desired pressure at ambient temperature using the syringe pump, capable of keeping constant pressure throughout the whole measurement process. As measurements took a very long time (up to 3 days), leakage had to be avoided. (It also could have influenced the results because of the Joule–Thompson effect.) After reaching an equilibrium, the measurement program could be started

on the calorimeter. The temperature programs used to study the three chlorinated mandelic acid derivatives and the phenylethanammonium salt of 4-chloromandelic acid differed. Their detailed description is to be found in the thesis.

2.3. Other measurement techniques applied in the research

The frame of the thesis booklet does not allow the detailed description of the atmospherical recrystallization and precipitation experiments, the capillary electrophoretic analyses conducted by CycloLab Ltd. and the atmospheric DSC and XRD measurements carried out at BME and at Ruhr-University Bochum. However, the detailed methods of these processes are listed in the thesis itself, as they compose a very important part of the research process.

2.4. Prediction of the liquidus curves in melting phase diagrams

Atmospheric differential scanning calorimetry (DSC) was used to confirm the previously known phase diagrams of the compounds. At ambient pressure, the Schröder–van Laar (1) and Prigogine–Defay equations (2) are commonly applied to model the melting phase behavior of enantiomeric (or diastereomeric) mixtures.¹⁰ However, the application of these relatively simple equations to predict the melting point of a mixture of a given composition under high pressure has not been demonstrated previously.

$$\ln X_R = \frac{\Delta H_{Rf}}{R} \cdot \left(\frac{1}{T_{Rf}} - \frac{1}{T_f} \right) \quad (1)$$

$$\ln 4X_R(1 - X_R) = \frac{\Delta H_{racf}}{R} \cdot \left(\frac{1}{T_{racf}} - \frac{1}{T_f} \right) \quad (2)$$

X_R denotes the mole fraction of the major enantiomer, ΔH_{Rf} and ΔH_{racf} denote the fusion enthalpies of the pure enantiomer and the racemate, respectively. R is the universal gas constant, T_{Rf} and T_{racf} are the melting temperatures of the pure enantiomer and the racemate, respectively. After reorganizing the equations, the predicted melting temperature T_f can be calculated. Melting point measurements (and predictions) are particularly interesting under supercritical carbon dioxide pressure because the depression in the melting point has been shown to be caused by the high pressure fluid dissolving in the solid material.¹¹ I aimed to investigate whether the Schröder–van Laar and Prigogine–Defay equations are able to describe the melting behavior of enantiomeric and diastereomeric mixtures under carbon dioxide

¹⁰ Q. He, J. Zhu, H. Goma, M. Jennings, S. Rohani, Identification and characterization of solid-state nature of 2-chloromandelic acid, *J. Pharm. Sci.* 98 (2009) 1835–1844. doi:10.1002/jps.21560.

¹¹ K. Fischer, M. Wilken, J. Gmehling, The effect of gas pressure on the melting behavior of compounds, *Fluid Phase Equilib.* 210 (2003) 199–214. doi:10.1016/S0378-3812(03)00180-8.

pressure. In case of the unreacted acids, the Prigogine–Defay equation was used to predict the liquidus curve at compositions between the racemate and the eutectic composition. Past the melting eutectic, the Schröder–van Laar equation was used. For the diastereomeric salts 1-phenylethanammonium-4-chloromandelate and 1-phenylethanammonium-mandelate, only the latter equation was used.

3. Results and discussion

3.1. Enantiomeric enrichment by the recrystallization of diastereomeric salts

As chiral resolution is often carried out via the formation of diastereomers, several times diastereomeric salts, it seems to be a very straightforward enantiomeric enrichment method to recrystallize said salts without the liberation of the target compound. The process was studied on the 1-phenylethanammonium salts of mandelic acid and 4-chloromandelic acid.

3.1.1. Comparison of recrystallization results and the melting phase diagram of 1-phenylethanammonium-mandelate

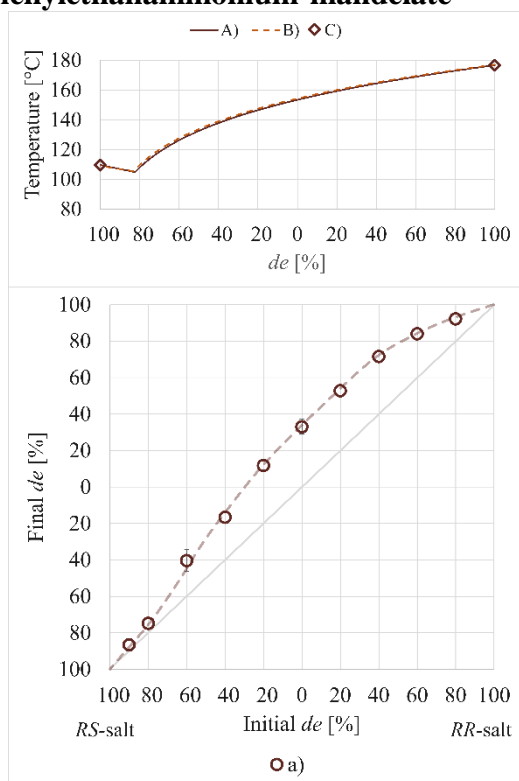


Figure 6 – Comparison of the melting phase diagram and recrystallization results of 1-phenylethanammonium mandelate a) Recrystallization experiments at 16 MPa, 99 mg/ml methanol concentration and 35 °C A) Melting phase diagram calculated based on measurements attempting to confirm the published melting properties of the diastereopure salts B) Melting phase diagram calculated based on literature data¹²; C) Melting points of the pure salts measured in the DSC

In the lower diagram of *Figure 6* the diastereomeric excess values of the raffinates of simulated recrystallization experiments are shown. The dashed line is not a fitted function, it only serves the purpose of guiding the eye. The measurement points are always located above the diagonal

¹² E.J. Ebberts, B.J.M. Plum, G.J.A. Ariaans, B. Kaptein, Q.B. Broxterman, A. Bruggink, B. Zwanenburg, New resolving bases for ibuprofen and mandelic acid: qualification by binary phase diagrams, *Tetrahedron: Asymmetry*. 8 (1997) 4047–4057. doi:10.1016/S0957-4166(97)00557-0.

line of the diagram. Using (*R*)-1-phenylethanamine, the crystalline product can be enriched in the *R* enantiomer of mandelic acid starting from any diastereomeric excess (except for the pure diastereomers, of course). The system does not clearly show a correlation between the melting phase diagram and the purification curve. However, a decrease in the enhancement of diastereomeric purity can be observed in the region of the melting eutectic composition, which suggests that the composition of the crystalline product might be thermodynamically influenced. This finding would be very counterintuitive. In antisolvent fractionation processes, the formation of the crystalline phase occurs rapidly as a result of high oversaturation. The very short time needed for the precipitation would theoretically favor the dominance of kinetic control.

3.1.2. Comparison between the purification results and the melting point phase equilibrium of the diastereomeric salt 1-phenylethanammonium-4-chloromandelate

Two series of GASF experiments were carried out in the full range from the diastereomerically pure and more soluble (*S*)-1-phenylethanammonium-(*R*)-4-chloromandelate to the less soluble (*R*)-1-phenylethanammonium-(*R*)-4-chloromandelate salt. The measurement series differed in the amount of organic solvent used to prepare the initial solutions.

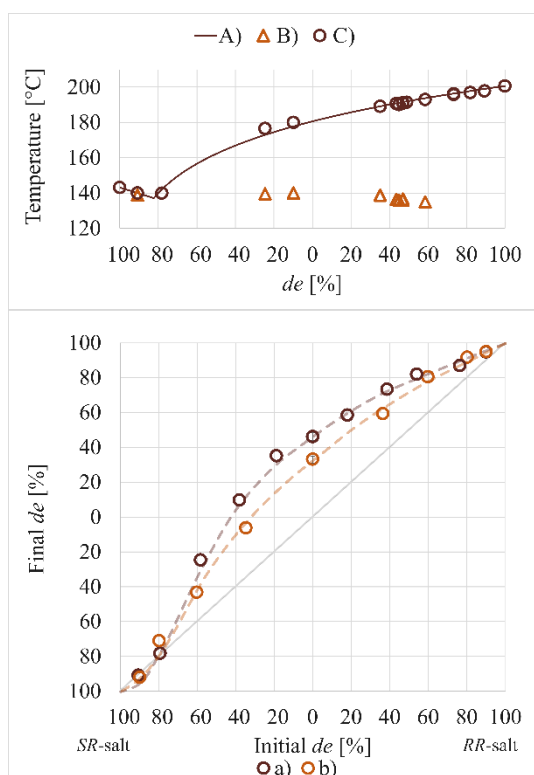


Figure 7 – Melting point phase diagram and final *de* vs. initial *de* diagram of the further purification experiments
a) Further purification experiments by GASF at 99 mg/ml methanol concentration
b) GASF experiments at 66 mg/ml methanol concentration;
A) Melting point curve calculated using the Schröder–van Laar equation;
B) Melting points registered as the onset of the first thermal event on the DCS curves, interpreted as eutectic melting;
C) Melting temperatures determined by the main melting peaks on the DSC curves

The results of the DSC melting point measurements and the prediction of the melting phase equilibrium shows a eutectic composition at approx. 80% diastereomeric excess of the *SR*-salt.

Observing the results of the GASF purification experiments a limiting composition is visible. Although the dashed curves are only drawn to guide the eye, their intersections with the diagonal reference line are confirmed by the closest measurement points. The limiting composition was found at approx. 80% *de* of the more soluble salt.

In addition to diastereomeric excess, yields are also important. Optimally, further purification would result in a large increase of *de* with maximal yield. The efficiency of diastereomeric enrichment (EDE^{13} , Figure 8.) is defined as the ratio of the enantiomeric purities of the product and the starting material multiplied by the yield. I compared the results of antisolvent experiments to atmospheric recrystallizations carried out in our own laboratory, at a very small scale and to some larger scale experiments done at ambient pressure described in the literature.

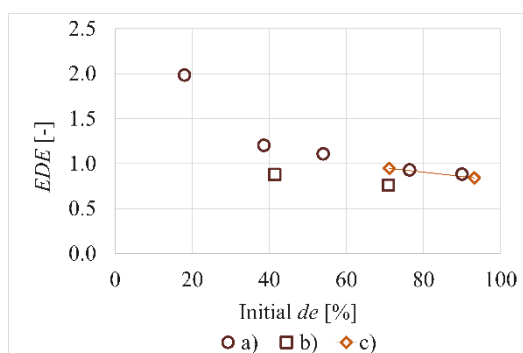


Figure 8 – Efficiency of diastereomeric enrichment (EDE) plotted against the initial *de*; a) GAS experiments on further purification; b) Atmospheric further purification experiments; c) Recrystallization experiments from the literature¹⁴

The EDE values of antisolvent experiments are higher than those of our own atmospheric measurements. This is not surprising regarding the latter recrystallizations' test tube-scale. Although, in terms of diastereomeric excess, the antisolvent experiments fall back compared to the recrystallizations done at ambient pressure, the EDE values are very similar to those calculated based on literature data. The explanation is that GASF yields slightly exceed the published atmospheric yields and significantly exceed those of our own atmospheric references. An upward trend of the yield with increasing initial diastereomeric excess was also observed, and is due to the increasing proportion of the less soluble salt in the solutions, with the overall salt concentration being constant as a function of initial *de*.

In order to gain a better insight into the effects and phenomena determining chiral separation in high pressure experiments, the melting phase diagram of the studied salt under carbon dioxide pressure was also recorded. High pressure DSC measurements could not be evaluated properly

¹³ $EDE = \frac{de_{product}}{de_{initial}} \cdot Y$, where Y is the yield.

¹⁴ H.E. Quan, Y.F. Peng, S. Rohani, Diastereomeric resolution of p-chloromandelic acid with (R)-phenylethylamine, *Chirality*. 22 (2010) 16–23. doi:10.1002/chir.20695.

in this case, as multiple thermal events were observed during runs, however, view cell experiments could be conducted. The results of these are shown in *Figure 9*.

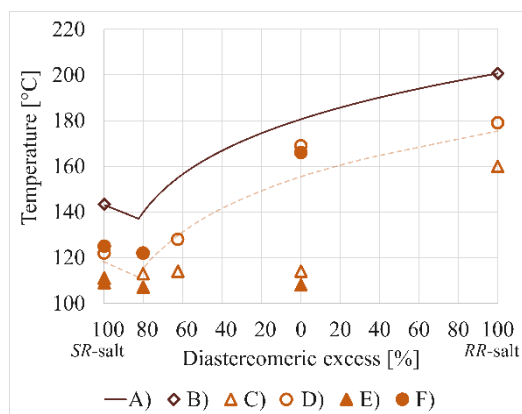


Figure 9 – Melting behavior of 1-phenylethanammonium 4-chlormandelate
 A) Predicted liquidus curve at ambient pressure
 B) Melting points measured in the atmospheric DSC equipment
 C) Temperature at the beginning of melting at 16 MPa; D) Temperature at the end of melting at 16 MPa; E) Temperature at the beginning of melting at 20 MPa; F) Temperature at the end of melting at 20 MPa

Initial melting temperatures do not show any clearly discernible tendency as a function of composition. Final melting temperatures correlate well with the atmospheric melting point curve, showing a similar eutectic behavior and eutectic composition. It can also be likely that the data points could be approximated using the Schröder–van Laar equation. However, without having properly measured input data, the equation could only be fitted to measured points. I intentionally avoided this step because of the relatively small

number of measurement points and the larger inaccuracies stemming from the visual measurement method.

3.2. Enantiomeric enrichment by the recrystallization of scalemic mixtures

It is known that non-racemic mixtures of enantiomers can be separated into fractions showing different enantiomeric compositions, even when using achiral separation processes. This phenomenon is called *self-disproportionation of enantiomers*. Gas antisolvent fractionation was applied in the recrystallization of the scalemic mixtures of 2-, 3- and 4-chloromandelic acids. Results were compared to the atmospheric melting phase diagrams of the same compounds.

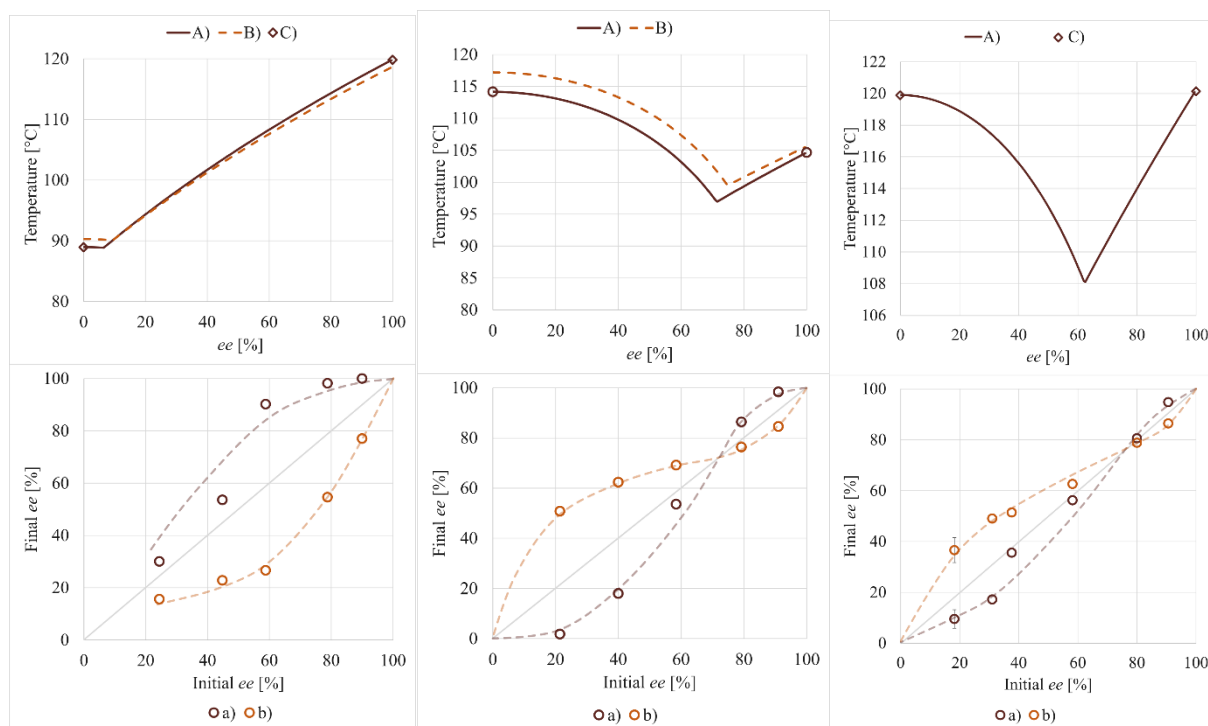


Figure 10 – Melting point phase equilibrium diagram (upper) and $ee_0 - ee_1$ diagram (lower) of 2-, 3- and 4-chloromandelic acid from left to right. A) Phase equilibrium curve modelled based on measured data; B) Melting liquidus curves calculated based on literature data¹⁵¹⁶; C) Melting points measured by atmospheric DSC experiments; a) Crystalline raffinates; b) Extracts

The results of the gas antisolvent fractionation experiments are shown in the lower sections of *Figure 10*. The dashed lines are drawn only to guide the eye. Non-ideal behavior is observed in all three diagrams, with two of the cases showing an intersection of the enantiomeric excess curves of raffinates (precipitated solids), extracts and the $ee = ee_0$ line. This is called the limiting composition, and is somehow similar to azeotropic compositions of binary liquid–vapor equilibrium curves. However, it must be noted that the enantiomeric excesses plotted in these diagrams are not compositions of phases in equilibrium, but initial and product enantiomeric excess values. Starting from a non-racemic mixture of any of the three acids, a crystalline raffinate and an extract can be produced, having different enantiomeric purities both from each other and from the starting material, if the initial ee is not equal to the limiting composition. This suggests that self-disproportionation of enantiomers occurs under the circumstances of the fluid-solid phase transition during GASF. The limiting compositions of 3- and 4-chloromandelic acid show strong correlations with the atmospheric melting eutectic

¹⁵ Q. He, J. Zhu, H. Goma, M. Jennings, S. Rohani, Identification and characterization of solid-state nature of 2-chloromandelic acid, *J. Pharm. Sci.* 98 (2009) 1835–1844. doi:10.1002/jps.21560.

¹⁶ Y. Zhang, A. Ray, S. Rohani, Measurement and prediction of phase diagrams of the enantiomeric 3-chloromandelic acid system, *Chem. Eng. Sci.* 64 (2009) 192–197. doi:10.1016/j.ces.2008.10.010.

compositions of the enantiomeric mixtures. The behavior observed at the two sides of the limiting composition is very similar to that observed in slow, atmospheric experiments conducted on thermodynamically controlled systems. This behavior suggests that the compositions of the separated products are dominated by an equilibrium.

As with 1-phenylethanammonium 4-chloromandelate, high pressure chiral melting phase diagrams were recorded (*Figure 11*) These measurements were done at Ruhr-University.

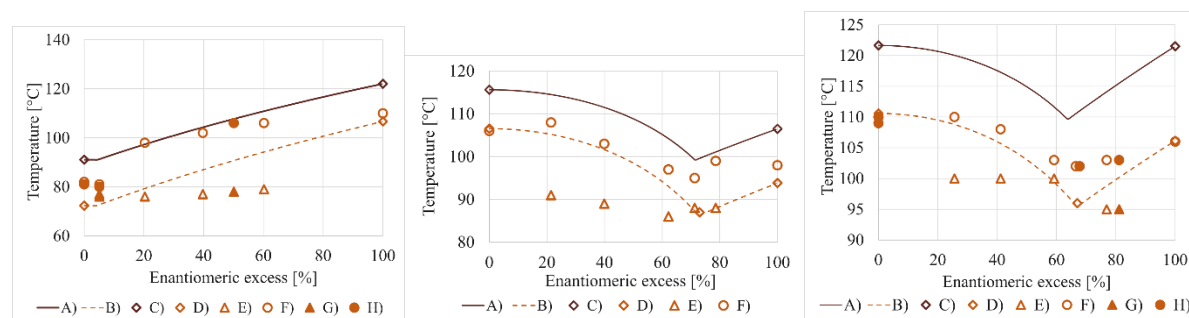


Figure 11 – Melting behavior of 2-, 3- and 4-chloromandelic acid (from left to right) at ambient pressure and under carbon dioxide. A) Calculated melting point curve at ambient pressure; B) Calculated melting point curve at 16 MPa; C) Melting points measured with atmospheric DSC; D) Melting points measured with high pressure DSC at 16 MPa; E) Beginning of melting observed in the view cell at 16 MPa; F) End of melting observed in the view cell at 16 MPa; G) Beginning of melting observed in the view cell at 20 MPa; H) End of melting observed in the view cell at 20 MPa

As high pressure DSC measurements could be successfully carried out on the acids (unlike on the diastereomeric salt), my goal was to investigate whether the Schröder–van Laar and Prigogine–Defay equations are able to describe the melting behavior of enantiomeric and diastereomeric mixtures under carbon dioxide pressure.

In order to confirm the calculated liquidus curves, melting experiments were conducted in the high pressure view cell at various enantiomeric compositions. Triangular markers correspond to the temperature at the observation of the first liquid droplet. These points approximate the eutectic melting temperature of the mixtures and – at 16 MPa – they are close to the eutectic (minimal) melting excess temperature predicted by the calculated phase diagrams in all of the three cases. In my opinion, measurement inaccuracy due to relatively rapid heating could explain the positive deviation from predicted values. In order to prove the accuracy of the eutectic melting temperatures, high pressure DSC measurements have been carried out at the predicted eutectic compositions of 3-chloromandelic acid and 4-chloromandelic acid at 16 MPa. The fact that only one melting peak could be observed suggests that the mixtures showed a eutectic behavior. The melting temperatures also match the predicted values at the corresponding pressures. Observing the final melting temperatures at 16 MPa (circular markers), one can conclude that their

tendencies follow the corresponding predicted melting point curve, showing minima at the predicted eutectic compositions. These findings show that using the Schröder–van Laar and Prigogine–Defay equations to describe the melting phase diagrams of chiral compounds is appropriate.

4. Thesis statements

1. Gas antisolvent fractionation has been applied for the first time in the recrystallization-based diastereomeric enrichment of 1-phenylethanammonium-mandelate and 1-phenylethanammonium-4-chloromandelate. In case of the diastereomeric salt of 4-chloromandelic acid, the efficiency of diastereomeric enrichment values have been compared to those calculated based on atmospheric experiments described in the literature, finding that a similar efficiency can be achieved. [I]; [III]
2. A detailed investigation on the recrystallization of the diastereomeric salts of enantiomerically pure 1-phenylethanamine and 4-chloromandelic acid of different enantiomeric excess values was carried out. A limiting composition was found in the product *de*–initial *de* curve. Said curve has been compared to the atmospheric melting phase diagram of the salt and a strong correlation between the limiting composition and the melting eutectic composition has been observed. [I]
3. I have been the first to observe *self-disproportionation of enantiomers* in the gas antisolvent fractionation process. I have demonstrated the phenomenon on the example of the scalemic mixtures of 2-, 3- and 4-chloromandelic acids. [II]
4. The product *ee*–initial *ee* curves of 2-, 3- and 4- chloromandelic acids have been recorded using gas antisolvent fractionation as a recrystallization method. Limiting compositions were identified in two cases (3- and 4-chloromandelic acid). Atmospheric chiral melting phase diagrams were recorded and compared to the purification diagrams. A correlation between the limiting composition in the purification curves and the melting eutectic composition in the atmospheric phase diagram has been observed for the first time. [II]
5. The influence of high pressure carbon dioxide on the chiral melting phase diagrams has been investigated for the first time, on the examples of 2-, 3- and 4-chloromandelic acid. I successfully proved the applicability of the Schröder–van Laar and Prigogine–Defay equations for the calculation of the liquid curve in the chiral melting phase diagrams under high pressure carbon dioxide. [IV]

5. Future considerations and applications

Although there are no known applications for the antisolvent precipitation–based enantiomeric enrichment, the green and non-hazardous nature of supercritical carbon dioxide and the possibility of lowering the use of organic solvents is promising. In cases where the size of the particles or the distribution of said particle size is important, high pressure antisolvent processes might become a viable alternative, especially if their products are directly applicable. For example, micronized materials offer a high specific surface area, which could be beneficial if the product is dissolved during its usage.

High pressure melting experiments have a relatively wide literature coverage, however, chiral temperature–composition phase diagrams have not been studied before. Besides providing a deeper insight into the interactions regulating the outcome of high pressure fractionation processes aiming chiral resolution, the measurements and results could help in understanding the behavior of other eutectic systems as well. In order to deepen our knowledge about high-pressure phase behavior and its correlation with antisolvent processes, a future plan – also being worked on at the time of writing the thesis – is to investigate the high pressure melting equilibrium in the presence of an organic co-solvent. This area requires new method development also, on which we are currently working.

Journal publications connected to the theses

- [I] M. Kőrösi, J. Madarász, T. Sohajda, E. Székely, Fast further purification of diastereomeric salts of a nonracemic acid by gas antisolvent fractionation, *Chirality*. 29 (2017) 610–615. doi:10.1002/chir.22730. (IF:1.833)
- [II] M. Kőrösi, J. Madarász, T. Sohajda, E. Székely, A fast, new method to enhance the enantiomeric purity of non-racemic mixtures: self-disproportionation of enantiomers in the gas antisolvent fractionation of chlorine-substituted mandelic acid derivatives, *Tetrahedron: Asymmetry*. 28 (2017) 1568–1572. doi:10.1016/J.TETASY.2017.09.005. (IF:2.377, Ind. Cit.:2)
- [III] M. Kőrösi, A. Sedon, K. Komka, T. Sohajda, E. Székely, Gas Antisolvent Fractionation: a New Method to Obtain Enantiopure Compounds, a Case Study on Mandelic Acid, *Period. Polytech. Chem. Eng.* 63 (2018) 130–137. doi:10.3311/PPch.11741. (IF:1.382)

[IV] M. Kőrösi, J. Béri, A. Hanu, S. Kareth, E. Székely, High-pressure melting equilibrium of chiral compounds: A practical study on chlorinated mandelic acids under carbon dioxide atmosphere, *J. CO₂ Util.* 37 (2020) 173–179. doi:10.1016/j.jcou.2019.11.026. (IF: 5.189)

Oral presentations

[1] M. Kőrösi, J. Béri, E. Varga, E. Székely, Enantiomerkeverék-továbbtisztítás gáz antiszolvens frakcionálással: a 3-klórmandulasav tisztíthatóságának és nagynyomású olvadási viselkedésének összevetése, XXV. International Conference on Chemistry, p. 42., Kolozsvár, Romania 2019

[2] M. Kőrösi, J. Béri, A. Hanu, M.-A. Wüstkamp, S. Kareth, E. Székely, The effect of carbon dioxide pressure on the melting phase equilibrium of chiral mandelic acid derivatives, 17th European Meeting on Supercritical Fluids- EMSF 2019., p. 76-77, ISBN: 978-84-09-10484-0, Ciudad Real: Institute of Chemical and Environmental Engineering, Spain 2019

[3] M. Kőrösi, J. Béri, J. Madarász, T. Sohajda, A. Hanu, S. Kareth, E. Székely, Enantiomeric enrichment by gas antisolvent fractionation, Applications of supercritical fluids, p. 10., ISBN 978-963-313-287-6 BME Department of Chemical and Environmental Process Engineering, Budapest, 2018

[4] M. Kőrösi, Nem-racém enantiomerkeverékek továbbtisztítása gáz antiszolvens frakcionálással, XV. PhD Conference of the György Oláh Doctoral School, Budapest University of Technology and Economics, 2018

[5] M. Kőrösi, J. Madarász, T. Sohajda, E. Székely, Enantiomeric enrichment by antisolvent fractionation of the diastereomeric salt 4-chloromandelic acid, 16th European Meeting on Supercritical Fluids-EMSF 2017., p. 81. ISBN 978-989-207-507-5 Lisbon: Universidade Nova de Lisboa, Faculdade de Ciências e Tecnologia, Portugal 2017

[6] M. Kőrösi, E. Székely, A. Zodge, T. Sohajda, 4-klórmandulasa resolválása és enantiomerkeverékeinek továbbtisztítása gáz antiszolvens kristályosítással, XXXIX. Kémiai Előadói Napok, p. 199., ISBN 978-963-9970-73-1, Szeged, Hungary, 2016

Poster presentations

- [7] M. Kőrösi, J. Madarász, T. Sohajda, E. Székely, Klórozott mandulasav származékok gáz antizsolvens frakcionálással történő átkristályosítása: egy új módszer nem racém enantiomerkeverékek továbbtisztítására, XIV. PhD Conference of the György Oláh Doctoral School, 46 p., Budapest University of Technology and Economics, 2017
- [8] Kőrösi M., Tárkányi M., Zodge A., Varga D., Sohajda T., Székely E., Chiral resolution in supercritical carbon dioxide: a background study on two carboxylic acids, Applications of supercritical fluids, p. 34., ISBN 978-963-313-179-4 BME Department of Chemical and Environmental Process Engineering, Budapest, 2015

Other publications

- [9] A. Zodge, M. Kőrösi, M. Tárkányi, J. Madarász, I. M. Szilágyi, T. Sohajda, E. Székely Gas Antisolvent Approach for the Precipitation of α -Methoxyphenylacetic Acid – (R)-1-Cyclohexylethylamine Diastereomeric Salt, Chem. Biochem. Eng. Q. 31 (2017) 335–341. doi:10.15255/CABEQ.2016.1023. (IF:1,383)
- [10] A. Zodge, M. Kőrösi, J. Madarász, I.M. Szilágyi, E. Varga, E. Székely, Gas Antisolvent Fractionation: A New Approach for the Optical Resolution of 4-chloromandelic Acid, Period. Polytech. Chem. Eng. 63 (2019) 303–311. doi:10.3311/PPCH.12910. (IF:1,382)
- [11] M. Kőrösi, J. Béri, A. Sedon, K. Komka, E. Székely, New vapour-liquid equilibrium data on the ternary system carbon dioxide – methanol – dimethyl sulphoxide, Fluid Phase Equilib. 497 (2019) 133–139. doi:10.1016/J.FLUID.2019.05.024. (IF:2,197)

Co-authorship in other conference presentations or posters

- [12] A. Zodge, M. Kőrösi, D. Hunyadi, I. Kmezc, J. Madarász, I. M. Szilágyi, T. Sohajda, E. Székely, Enantioselective diastereomeric salt formation of 4-chloromandelic acid with (R)-(+)- α -Phenylethylamine in supercritical CO₂, 15th European Meeting on Supercritical Fluids, Essen, Germany, 2016
- [13] A. Zodge, M. Kőrösi, I. Kmezc, J. Madarász, T. Sohajda, E. Székely, Gas antisolvent precipitation of 4-chloromandelic acid with (R)-(+)- α -Phenylethylamine and (R)-1-cyclohexylethylamine in supercritical CO₂, 15th European Meeting on Supercritical Fluids, Essen, Germany, 2016

- [14] E. Székely, M. Zsemberi, L. Lőrincz, M. Kőrösi, A. Zodge, T. Sohajda, J. Madarász, Towards pure enantiomers with supercritical carbon dioxide based crystallizations, 22nd International Congress of Chemical and Process Engineering, CHISA 2016 and 19th Conference on Process Integration, Modelling and Optimisation for Energy Saving and Pollution Reduction, p. 683-684., ISBN 978-151-085-962-3, PRES, Prague 2016
- [15] A. Zodge, M. Kőrösi, M. Tárkányi, J. Madarász, I. M. Szilágyi, S. Boyajiev, T. Sohajda, E. Székely, Influence of pressure on antisolvent precipitation and particle shapes, Applications of supercritical fluids, p. 20., ISBN 978-963-313-179-4, BME Department of Chemical and Environmental Process Engineering, Budapest, 2015
- [16] A. Zodge, M. Kőrösi, M. Tárkányi, D. Hunyadi, P. Bombicz, J. Madarász, I. M. Szilágyi, T. Sohajda, E. Székely, Enantioselective diastereomeric salt precipitation of 2-Methoxyphenylacetic acid using (*R*)-1-Cyclohexylethylamine with supercritical carbon dioxide, 10th European Congress of Chemical Engineering - 3rd European Congress of Applied Biotechnology - 5th European Process Intensification Conference: ECCE10+ECAB3+EPIC5., Nice, France 2015
- [17] A. Zodge, M. Kőrösi, J. Dingemans, E. Székely, Supercritical antisolvent precipitation for separation of enantiomers, 52nd EHPRG Meeting, Lyon, France, 2014

